Available online at www.sciencedirect.com
ScienceDirect
Polymer 48 (2007) 5279–5288
polymer
www.elsevier.com/locate/polymer

Spectroscopic evidence for the bulk polymerization of *N*-vinyl carbazole in the presence of single-walled carbon nanotubes

Mihaela Baibarac [a,*], Ioan Baltog [a], Serge Lefrant [b], Pedro Gomez-Romero [c]

[a] *National Institute of Materials Physics, Laboratory of Optics and Spectroscopy, R-77125 Bucarest – Magurele, P.O. Box MG-7, Romania*
[b] *Institut des Matériaux Jean Rouxel, 2 rue de la Houssinière, B.P. 32229, 44322 Nantes, France*
[c] *Institut de Ciència de Materials de Barcelona, Campus de la UAB, 08193 Bellaterra, Spain*

Received 14 April 2007; received in revised form 3 July 2007; accepted 4 July 2007
Available online 12 July 2007

Abstract

The bulk polymerization reaction of *N*-vinylcarbazole (VK) at 70 °C in the presence of single-walled carbon nanotubes (SWNTs) leads to a new composite, whose optical properties were studied by photoluminescence (PL), surface enhanced Raman scattering (SERS) and Fourier transform infrared (FTIR) spectroscopies. A dramatic reduction of the poly(*N*-vinylcarbazole) (PVK) PL efficiency and a change in the vibrational structure of the PL spectrum of this polymer were observed by adding SWNTs to the synthesis mixture. Steric hindrance effects were evidenced both in SERS spectra of the VK when it interacts mechanico-chemically with SWNTs and in FTIR spectra of the un-doped PVK/SWNTs' composites. Cyclic voltammetry was used to demonstrate the doping process of PVK in PVK/SWNTs' composite.

Keywords: Nanocomposites; Carbon nanotubes; SERS spectroscopy

1. Introduction

In recent years, increasing attention has been devoted to poly(*N*-vinylcarbazole)/carbon nanotubes (PVK/CNs) nanocomposites [1–8], as a result of a number of interesting physical and chemical properties such as: (i) optical limiting performance [1,2], (ii) good photoconductivity [1,3], (iii) potential use as an active material in rechargeable batteries and supercapacitors [5], (iv) fabrication of light emitting devices based on SWNTs/PVK composites [6] and (v) multi-walled carbon nanotubes used as mechanical reinforcement agent in PVK [8]. For PVK/CNs nanocomposites, three synthesis methods have been reported so far: (i) a direct mixing of the polymer with nanotubes in chloroform, (ii) a chemical polymerization of the monomer in the presence of CNs and butyllithium and (iii) an electropolymerization of VK on a CN film via cyclic voltammetry in $LiClO_4$/acetonitrile solution [1–8]. In this paper, a new synthesis route for the PVK/SWNTs' composites is reported.

Although several papers are devoted to the physico-chemical properties of SWNTs and their polymeric derivatives [9,10], little attention has been paid to the functionalization of SWNTs by the bulk polymerization of electron-rich monomers such as *N*-vinyl carbazole (VK). Earlier studies by Biswas and Haque concerning the polymerization of VK on carbon black (CB) proposed a direct initiation mechanism by an electron transfer between the two components [11,12]. Later, a report by Chen et al. described the polymerization of VK, initiated by fullerenes in bulk at 70 °C (melting temperature of VK is 65 °C) as taking place via C_{60}-VK ion-radical pairs [13]. With this background, we tried in this work to elucidate whether a functionalization of nanotubes takes place or not in the case of the VK/CNs synthesis mixture. For this, comparative Raman studies were performed on samples obtained by (i) bulk polymerization of VK in the presence of carbon nanoparticles of the types, SWNTs and C_{60} and (ii) mechanico-chemical reactions carried out with

---

* Corresponding author. Tel.: +40214930195; fax: +40214930267.
E-mail address: barac@infim.ro (M. Baibarac).

0032-3861/$ - see front matter © 2007 Elsevier Ltd. All rights reserved.
doi:10.1016/j.polymer.2007.07.008

different VK and SWNTs' mixtures. When preparing a composite, it is essential to determine the type of interaction between the host matrix and the guest nanoparticles. It is generally accepted that there are two main approaches for the surface modification of CNs [14]: one involves a non-covalent attachment of molecules while the second is a covalent attachment of functional groups to the CNs walls. In this work, SERS and FTIR spectroscopic studies are used to examine the attachment type. The different behavior of SWNTs, metallic and semiconducting, in the polymerization process is revealed by the Raman studies at excitation wavelengths of 676.4 and 1064 nm, respectively. In addition, the photoluminescence properties of these new composite materials are discussed. Further proofs supporting the proposed molecular structure of the PVK/SWNTs' composite obtained by bulk polymerization are provided by cyclic voltammetry.

2. Experimental part

According to Ref. [15], the bulk polymerization of VK leads to a white powder in contrast to the deeply coloured PVK usually resulting when a charge transfer polymerization system is used. The conversion of VK to PVK was determined to be ca. 20% in the case of bulk polymerization [16]. The bulk polymerization reaction of VK in the presence of SWNTs was carried out in a manner similar to that reported in Ref. [15], namely, under purified dry argon. Thus, VK (0.5 g) was mixed by grinding thoroughly with a known weight of CNs powder (0.1, 0.05 and 0.01 g), and the reaction mixture placed in a 50 ml conical flask was then heated to about the melting point of VK for 4 h. To stop the bulk polymerization, a known volume of tetrahydrofuran (10 ml) was added. Afterwards the contents were added to an excess of methanol. The resulting separated mass was filtered and washed repeatedly with boiling methanol to remove the un-reacted monomer and adhering substance. Each filtration of the PVK/SWNTs' suspension was preceded by an ultrasonic treatment for a few minutes. Washing with THF was carried out in order to separate the un-grafted PVK on SWNTs. The grey-black coloured residue (PVK-functionalized SWNTs) was dried at 50 °C under vacuum for 3 h to attain constant weight. Using the same polymerization time and by increasing the carbon nanotubes weight from 0.01 to 0.05 and 0.1 g at the synthesis mixture, a PVK/SWNTs' composite total mass of ca. 0.23, 0.36 and 0.52 g is obtained. The estimated percentage of PVK in the composite mass is of ca. 44, 62 and 84%.

For PVK/C_{60} composite synthesis, the procedure described in Ref. [13] was used.

All compounds used in this paper, i.e. VK, SWNTs, C_{60} and PVK were purchased from Sigma–Aldrich. The purity of VK and SWNTs was of 98% and $\geq$90%, respectively. Additionally, VK was twice re-crystallized from methanol at 40 °C, freeze-dried, and stored in vacuum and in dark before use. The purification of SWNTs was carried out by cyclic voltammetry using a 0.5 M HCl solution and post-treatments with alkaline solutions according to Ref. [17].

Photoluminescence (PL) spectra at room temperature were obtained under 265 nm light excitation emitted from a 150 W high pressure xenon lamp in a right angle geometry using a computer-controlled emission spectrometer consisting of a SPEX double monochromator equipped with a cooled EMI photomultiplier and a photon counting system.

SERS spectra were recorded at room temperature in a backscattering geometry with excitation wavelengths of 676.4 and 1064 nm using (i) a Jobin Yvon T64000 Raman spectrophotometer equipped with a microprobe allowing focusing of the laser spot onto the sample within a micrometer scale and (ii) a FT Raman Bruker RFS 100 spectrophotometer, respectively. For SERS measurements, films of about 100 nm thickness deposited on Au substrates with a rough microstructure in the range of 10–100 nm were used [18].

Fourier transformed-infrared (FTIR) spectra, in the range 400–4000 cm^{-1} with a 4 cm^{-1} resolution, were obtained using a Perkin–Elmer model 683 instrument.

The electrochemical doping process of the composite based on SWNTs and PVK in un-doped state was performed by cyclic voltammetry (CV), in the potential range (0; +1.8) V vs. Ag/AgCl in a conventional three electrode one-compartment cell. The working electrode was a PVK/SWNTs' film on a Pt plate (1 cm^2), deposited by evaporation from a composite solution (0.1 wt% in toluene). The counter electrode consisted of a spiral Pt wire. The potential of the working electrode was measured by reference to $\mathrm{Ag/Ag^+}$. The electrolyte used in this case was a solution of 10^{-1} M $\mathrm{LiClO_4}$ in acetonitrile (AN). The electrochemical doping process was performed using a potentiostat/galvanostat from Princeton Applied Research model 273A.

TEM images of SWNTs and the PVK/SWNTs' composite were recorded with a JEOL 1210 electron microscope operating at 120 kV.

3. Results and discussion

Fig. 1 shows PL spectra of samples obtained by bulk polymerization of VK in the absence (curve 1) and presence of SWNTs (curves 2–5). A first proof that the bulk reaction of VK at 70 °C corresponds to a polymerization is that its PL spectrum is identical to that obtained from an authentic PVK sample obtained from Aldrich–Sigma (spectrum 1, Fig. 1). As observed in Fig. 1, the PL spectrum of PVK consists of a band with a maximum around 3.02 eV (410 nm) that has been formerly assigned to the low-energy excimer [19]. The inset in Fig. 1 shows the variation of the ratio Φ_F^0/Φ_F (Φ_F^0 and Φ_F are the intensities of the photoluminescence of PVK alone and PVK-functionalized SWNTs, respectively) as a function of the mass of SWNTs (g) used in the synthesis of PVK/SWNTs' composite. A dramatic reduction of the PVK PL efficiency is observed when SWNTs are added to the synthesis mixture. The increase of absorbance for the exciting light, due to the presence of the SWNTs, is probably the main explanation for the decrease of PL intensity in this new composite. However, the appearance of a new emission band at ca. 2.48 eV (500 nm) indicates an electronic interaction between components. This may explain the decrease of the PL intensity as resulting from a quenching effect at the polymer/carbon nanotube interface. A possible quenching mechanism can be the

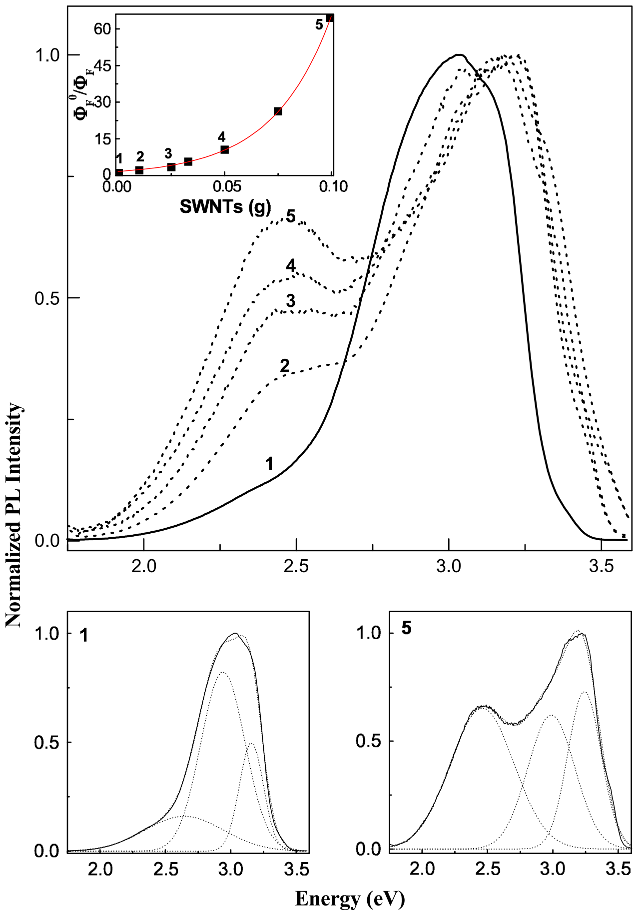

Fig. 1. PL spectra of compounds obtained by bulk polymerization of VK (0.5 g) in absence (curve 1) and presence of different amounts of SWNTs: 0.01 g (curve 2), 0.025 g (curve 3), 0.05 g (curve 4) and 0.1 g (curve 5).

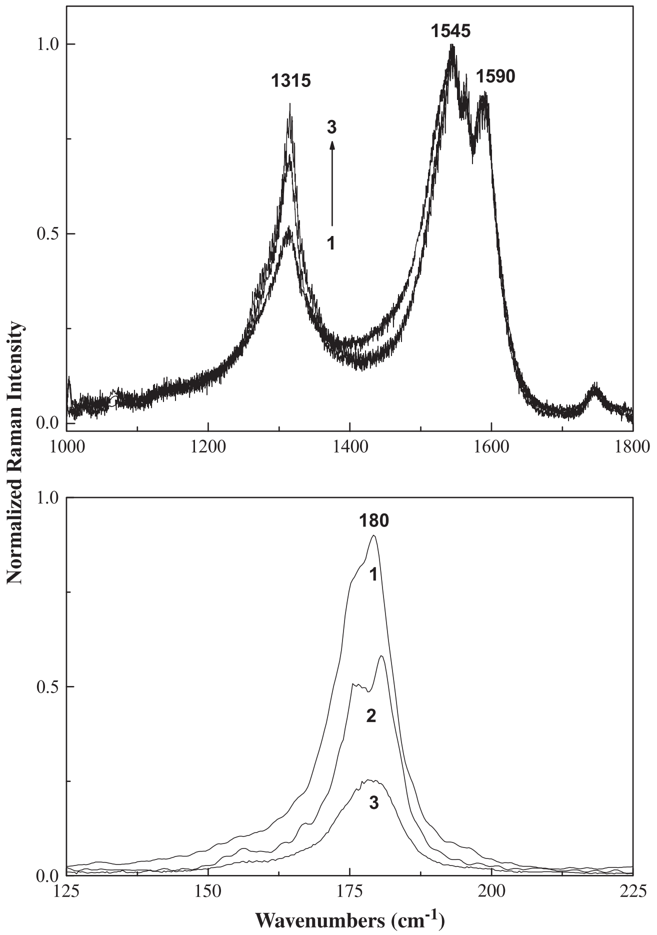

Fig. 2. SERS spectra at $\lambda_{exc} = 676$ nm of SWNTs' films of about 100 nm thickness deposited on the rough Au support (curve 1) and composites obtained by the bulk polymerization of VK (0.5 g) in the presence of different amounts of SWNTs: 0.01 g (curve 2) and 0.1 g (curve 3).

transfer of electron–hole pair (excitons) generated in PVK chains to SWNTs, in other words an energy transfer, similar to those reported for poly(*p*-phenylene vinylene)/multi-walled carbon nanotubes (PPV/MWNTs) composite [20]. The plots 2–5 in Fig. 1 show significant changes in the vibrational structure of the PL spectra of PVK resulting from the addition of SWNTs to the synthesis mixture. In this context, we note the shift of the PL band from 410 nm (3.02 eV) to 385 nm (3.22 eV) and the appearance of a new PL band around 500 nm (2.48 eV) which grows in intensity with the amount of SWNTs. It may be relevant to mention that a similar effect was reported for PPV/MWNTs composites [20]. At the first sight, the shift of the PL band from 3.02 at 3.22 eV seems to lead to the conclusion that the PVK/SWNTs' composite contains rather shorter polymer chains, of oligomer type. On the other hand in the particular case of the PL spectra of PVK, the emission bands at 385 nm (3.22 eV) and 410 nm (3.02 eV) are considered originating from the excimers formed in the partially eclipsed and fully eclipsed configuration of PVK, respectively [21]. According to this, we are tempted to interpret the variation of PL spectra of PVK/SWNTs' composite as a function of SWNTs' weight, as resulting from a random bonding of PVK molecules on the tube wall, which favors the formation of a partially eclipsed structure. The band peaked at 2.48 eV, increasing with the SWNTs' content, indicates the formation of a new luminescent center, which can be a defect induced in the macromolecular chain by the covalent bonding of SWNTs.

A further argument supporting the idea that the bulk polymerization reaction of VK in the presence of SWNTs involves a functionalization process of CNs with PVK is obtained by SERS spectroscopy. In the following, SERS spectra of nanotubes before and after the bulk polymerization reaction of VK are presented. Figs. 2 and 3 show SERS spectra of SWNTs' films at excitation wavelengths 676 and 1064 nm, respectively. Spectra exhibited the well-known two main groups of bands whose relative intensities and peak positions vary with excitation wavelength. The first group, from 100 to 350 cm^{-1} is associated with the radial breathing modes (RBM). The intensity and peak position of these bands, related to the tube diameter through the relation ν (cm^{-1}) = 223.75/d (nm) [22], are very sensitive to the excitation wavelength. The two strong bands situated at 176 and 164 cm^{-1}, observed at excitation wavelengths of 676 and 1064 nm, indicate that resonance occurs over a narrow range of diameters of about 1.36 and 1.27 nm, respectively. At the excitation wavelength of 1064 nm, the two Raman lines at 164 and 176 cm^{-1} have been associated with the RBM activated in isolated and bundled nanotubes, respectively [23]. The second

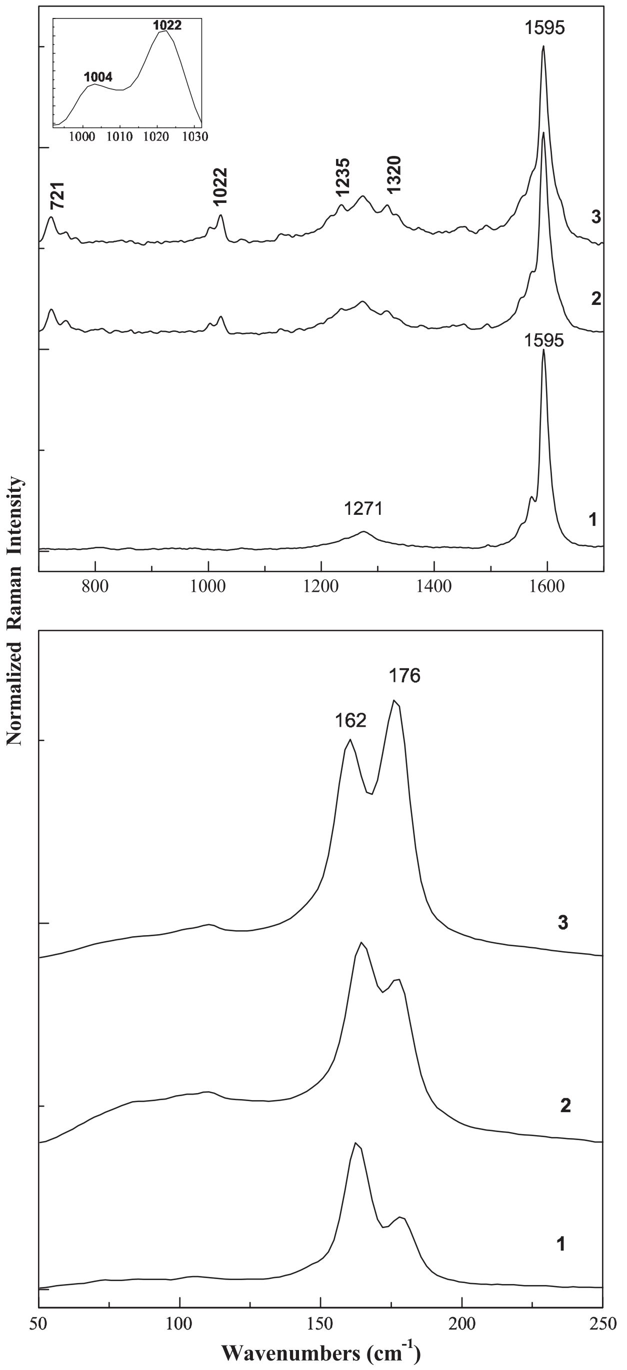

Fig. 3. SERS spectra at $\lambda_{exc.} = 1064$ nm of SWNTs' films of about 100 nm thickness deposited on the rough Au support (curve 1) and composites obtained by the bulk polymerization of VK (0.5 g) in the presence of different amounts of SWNTs: 0.01 g (curve 2) and 0.1 g (curve 3).

group, consisting of the TM and D bands, is found from 1000 to 1700 cm^{-1}. These bands are not only related to the nanotube structure; the former, peaking at about 1595 cm^{-1} and attributed to the tangential vibration mode, is also seen in the Raman spectra of other graphitic materials such as HOPG [24]. Analysis of the group of bands associated with TM vibrations at 676 nm excitation wavelength reveals four components, three of Lorentzian type at about 1606, 1588 and 1560 cm^{-1}, with widths at half maximum of about 32, 26 and 26 cm^{-1} and the fourth, at about 1542 cm^{-1}, asymmetrical in its lower energy side with a Breit–Wigner–Fano profile indicating an electron–phonon interaction [25,26]. The D band is frequently associated with a disorder in the graphitic lattice or defects in nanotubes [22,27].

The main changes observed in the Raman spectra of SWNTs as a result of the bulk polymerization of VK consist of (i) a stronger decrease in the intensity of the Raman bands in the 125–225 cm^{-1} spectral range, accompanied by an increase in the intensity of the D band without any other modification in the profile of the TM band at the excitation wavelength of 676 nm (Fig. 2); (ii) at an excitation wavelength of 1064 nm, besides the increase in the intensity of the D band, one also observes a modification in the intensity ratio of the Raman lines situated at 162 and 176 cm^{-1} in favour of the latter (Fig. 3). This indicates a decrease in the relative proportion of isolated tubes as a result of interaction between the polymer and individual SWNTs. In this case, the appearance of new Raman peaks at ca. 721, 1022, 1235 and 1320 cm^{-1} is clearly noted in spectra 2 and 3 of Fig. 3. As it is observed in Fig. 4, all these new Raman bands are identified in Fig. 3 as belonging to the SERS spectrum of PVK.

We note that the SERS spectrum of PVK, obtained by the bulk polymerization of VK in the absence of carbon nanotubes, is identical regardless of the excitation wavelength used, i.e. 676.4 or 1064 nm. The locations of the experimentally observed Raman lines and their attributions are summarized in Table 1 [28]. For composites prepared by bulk polymerization

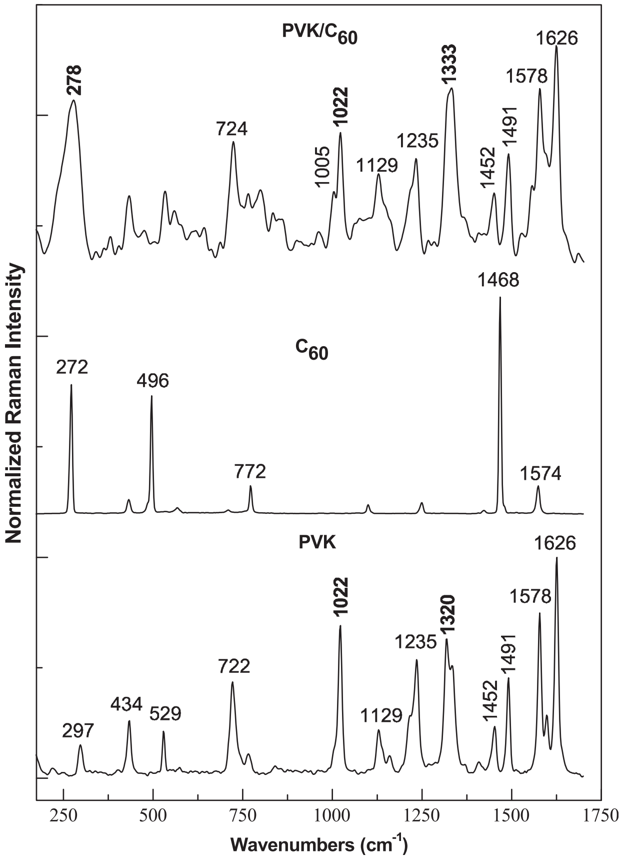

Fig. 4. SERS spectra at $\lambda_{exc.} = 1064$ nm of the PVK, C_{60} and PVK/C_{60} films of about 150 nm thickness deposited on the rough Au support.

Table 1
Vibration modes observed by surface enhanced Raman scattering spectroscopy in PVK, PVK/C_{60} and PVK/SWNTs

PVK [27]	PVK/C_{60}	PVK/SWNTs	Assignments [27]
297			C–C deformation in polyvinyl
434; 529			Benzene ring deformation
722	724	721	Rocking–wagging of methylene in polyvinyl
	1004	1004	
1022	1022	1022	Rocking–twisting of methylene in polyvinyl
1129	1129		Rocking–twisting of methylene in polyvinyl
1235	1235	1235	Wagging of methylene in polyvinyl
1320	1333	1320	C–H deformation of benzene ring
1452	1452		C–H in hetero-five member ring
1491	1491		Stretching of hetero-five member ring
1578	1578		C=C stretching in benzene ring
1626	1626		C–C stretching in benzene ring

of VK in the presence of SWNTs, we observe in the 1000–1030 cm^{-1} spectral range, the appearance of a new band with a maximum at about 1004 cm^{-1} of intensity nearly equal to those of Raman line peaking at 1022 cm^{-1} (Fig. 3, curves 2 and 3). A puzzling fact is that the same Raman band at 1004 cm^{-1} is also observed on the SERS spectrum of the PVK/C_{60} composite prepared by bulk polymerization (Fig. 4). In this last case, it is worth noting that this band is not detected in the SERS spectrum of the C_{60} film (Fig. 4) [29]. At first sight, it is attractive to consider the Raman line at about 1004 cm^{-1} as a characteristic signature of the chemical interaction between methylene groups and different carbon nanoparticles such as SWNTs and C_{60}. At this stage, a correct assignment of this Raman band is difficult. However, if the above statement is true, then one way to more thoroughly investigate the origin of the Raman line at ca. 1004 cm^{-1} might be via a mechanico-chemical process using VK as the host matrix and SWNTs as guest particles.

We point out that mechanico-chemical processes consist of chemical reactions which are controlled by mechanical motion/energy. We also note that solid-phase mechanico-chemical reactions involve highly reactive centres generated by the mechanical energy imparted to the reaction system. A good example in this sense is the reaction between SWNTs and KOH [30].

According to an early paper, the main Raman lines of VK are situated at: 220, 431, 569, 743, 1015, 1107, 1291, 1314, 1455, 1576, 1629 and 1640 cm^{-1} [30]. The Raman line at 1640 cm^{-1} is attributed to vinyl group [31]. Observing these lines, we notice that the transition from the monomer (VK) to the polymer (PVK) is noticed by: (i) a down-shift of the Raman line from 743 to 722 cm^{-1}; (ii) an up-shift of the Raman lines from 1107 and 1314 cm^{-1} to 1129–1138 and 1320 cm^{-1}, respectively, and (iii) a disappearance of the Raman line peaked to 1640 cm^{-1}. According to the data presented in Refs. [28,31] , the Raman lines peaking at 722, 1129, 1320 and 1640 cm^{-1} can be attributed to the following vibrations modes: rocking–wagging of methylene in polyvinyl, rocking–twisting of methylene in polyvinyl, C–H deformation of benzene ring and vinyl group, respectively. In the case of VK alone compressed for 5 min. at 0.58 GPa, the SERS spectrum (Fig. 5) shows the following features: (i) an intense Raman band at 718 cm^{-1} associated to the vibration of rocking–wagging of methylene in polyvinyl; (ii) a well developed Raman band at 1320 cm^{-1} attributed to the vibration C–H deformation of benzene ring; (iii) the appearance of a new Raman line at 1370 cm^{-1}; and (iv) in the 1000–1030 cm^{-1} spectral range we found a complex Raman band having two components at about 1004 and 1022 cm^{-1}. In addition, we observe that the intensity ratio between the two Raman lines (I_{1004}/I_{1022}) is around 1.5. In our opinion according with Scheme 1 the band at 1004 cm^{-1} can be associated to the ring breathing vibration mode of cyclobutane. At the first sight the formation of cyclobutane can be considered as a speculation of the logical analysis. However, an inspection of the basic data concerning the Raman characteristics of organic molecules reveals a Raman band at 1001 cm^{-1} attributed to the ring breathing vibration of cyclobutane [32]. We notice that a similar scheme was proposed for the polystyrene-bound C_{60} gel [33]. The appearance of the Raman bands at 718 and 1004 cm^{-1} confirm that by compression, an addition reaction of VK molecules takes place.

The simultaneous presence of the 1640 cm^{-1} line in the SERS spectrum of compressed VK indicates that a part of VK remains un-reacted. According to our expectation, a modification of the intensity ratio between the Raman lines at 1004 and 1022 cm^{-1} is observed when VK is compressed in the presence of SWNTs. As the proportion of SWNTs in the VK/CNs mixture increases from 1 to 10 wt%, the I_{1004}/I_{1022} ratio value changes to 1 and 0.5, respectively. Other changes observed in Fig. 5 are (i) the appearance of a Raman line with the maximum at 180 cm^{-1}, which becomes the most intense line in the Raman spectrum when SWNTs = 10 wt% in the VK/CNs mixture; (ii) a gradual increase in the intensity of the Raman line peaking at 1320 cm^{-1} as the SWNT fraction in the VK/CNs mixture is increased; and (iii) a decrease of the intensity down to complete disappearance of the Raman lines at 1370 and 1640 cm^{-1}. The above mentioned facts indicate that during compression, SWNTs perturb both the benzene ring and the vinyl group of VK. Another remark regards the presence of the Raman line at 180 cm^{-1}, associated to RBM of SWNTs in bundles – this confirms the additional roping of the isolated CNs in the presence of VK.

In order to better illustrate our hypothesis on the processes involved, we postulate the four products to be generated on VK compression alone or in the presence of SWNTs (Scheme 1). We note that Scheme 1 explains the following experimental facts: (i) the presence of the Raman band at 718 cm^{-1} in compressed VK sample is as a result of an addition reaction; (ii) for the compressed VK/SWNTs' mixture, the presence of the Raman lines at 718 and 1004 cm^{-1} indicates the chemical interaction of CNs with the vinyl group; (iii) the enhancement of the Raman band intensity at 1320 cm^{-1} in the compressed VK/SWNTs' mixtures could be explained as a result of steric hindrance effect induced by the benzene ring of VK as a consequence of the formation of new covalent bonds between CN

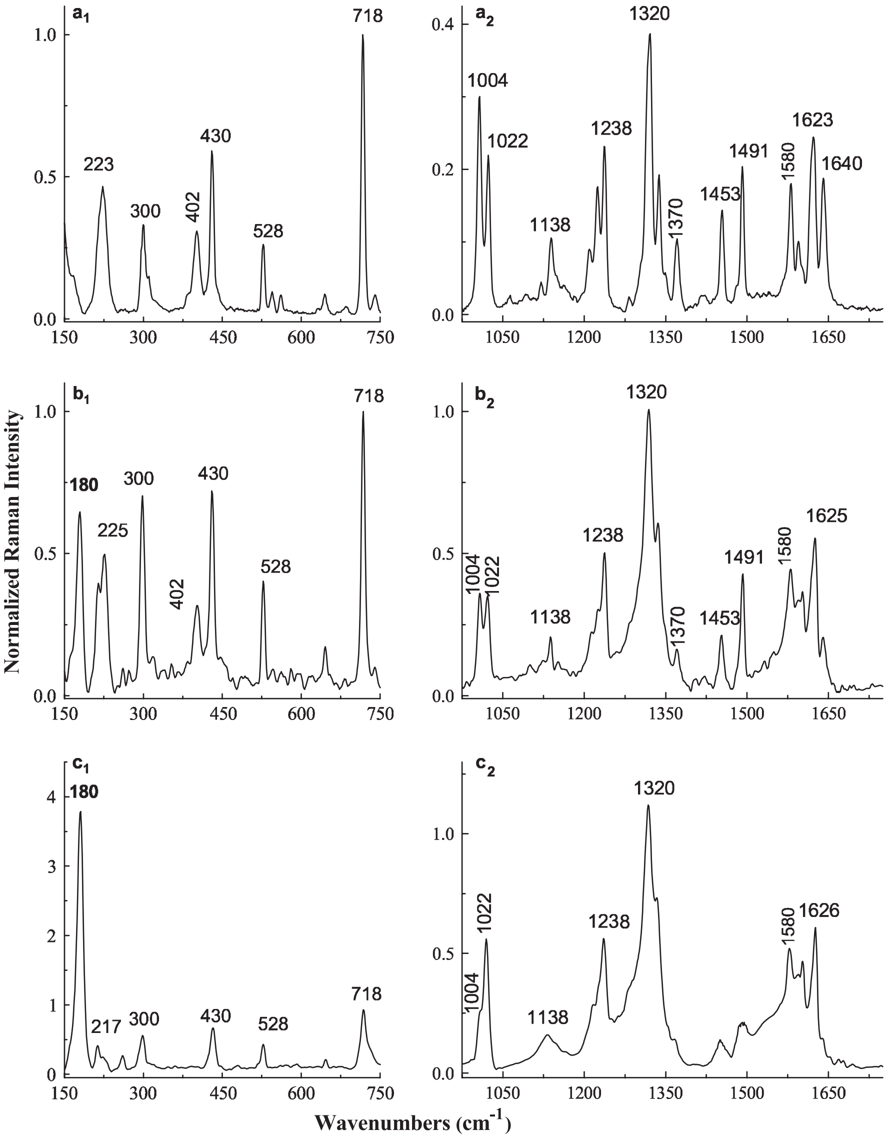

Fig. 5. SERS spectra at $\lambda_{exc.} = 1064$ nm of VK after its compression at 0.58 GPa alone (a_1, a_2) and in the presence of the 1 (b_1, b_2) and 10 (c_1, c_2) wt% SWNTs.

and the aromatic structure of VK; (iv) the absence of the Raman line at 164 cm^{-1} associated with the vibration of RBM of isolated SWNTs and the presence of an intense Raman band at 180 cm^{-1} attributed to the RBM of bundled CNs confirm the additional roping of isolated nanotubes. We think that the intense roping process invoked for mechanico-chemical reactions carry out on the VK/SWNTs' mixture (Fig. 5) in comparison with those reported during the bulk polymerization of VK in the presence of CNs (Fig. 3) has its origin in the appearance of tubes' fragments as demonstrated in a recent paper [34]. According with the studies of Strano et al. [35], the enhancement of the Raman band at 180 cm^{-1} could be regarded also as signature of SWNTs' aggregates. However, between the two processes that could lead to an enhancement of the Raman band at 180 cm^{-1}, some differences may exist resulting from the nature of driven forces. In the first case, for the functionalization of SWNTs, stronger forces are involved resulting from the covalent bounding while in the later case, weak forces of van der Waals type acts. The stronger forces involved in the functionalization of SWNTs induce significant changes in the FTIR spectrum of PVK/SWNTs' composite in comparison with the FTIR spectrum of PVK alone, Fig. 6. In addition, analyzing the Raman spectrum of the PVK/C_{60} composite, displayed in Fig. 4, the fact that the band at 278 cm^{-1} associated to the radial vibration mode $H_g(1)$ of C_{60} fullerenes is up-shifted in comparison with its normal position ($\sim$269 cm^{-1}) and much enhanced with respect of other Raman bands is very suggesting. This behavior is quite similar to what is observed for the band 180 cm^{-1} associated to the RBM of bundled CNs. In the case of C_{60} fullerenes, an aggregation process is revealed in the Raman spectrum by distinct signatures dependent on the strengthening of the forces involved: (i) when weak forces of van der Waals type are involved, the aggregation is similar to a process of precipitation of C_{60} into strong and poor solvent mixture, yielding C_{60} clusters whose Raman spectrum remains unchanged; (ii) when self-assembling C_{60} is driven by strong forces originating in charge transfer, the Raman

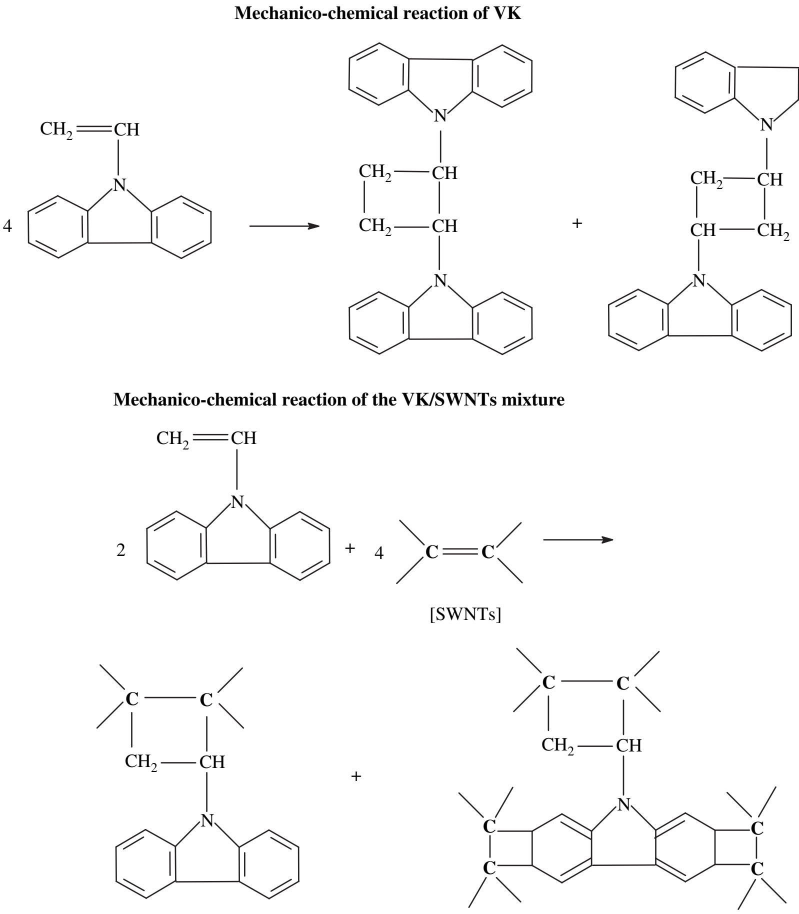

Scheme 1. Mechanico-chemical reactions of VK alone and the VK/SWNTs' mixture.

spectrum reveals a significant decrease of the intensity of $H_g(1)$ band that down-shifts to 255 cm^{-1} and the appearance of a new band at ca. 93 cm^{-1} [29]. Returning to Fig. 4, we notice that in the case of PVK/C_{60} composite, the enhancement of the band associated to the $H_g(1)$ mode and its up-shift at 278 cm^{-1} is a new experimental fact, different to that already observed in the case of C_{60} self-assembled. Such a result can be considered as a consequence of the functionalization of C_{60} with PVK that is different from an aggregation process. Similarly, in the case of PVK/SWNTs' composite, we tentatively explain the enhancement of the band at 180 cm^{-1} as resulting from a functionalization of SWNTs with PVK.

With all this in the mind and returning at Fig. 3, we can invoke a covalent functionalization of SWNTs with un-doped PVK. Two experimental techniques can support this hypothesis: FTIR spectroscopy and cyclic voltammetry. Fig. 6 shows FTIR spectra of PVK alone (prepared by bulk polymerization) and of two composites obtained by the bulk polymerization of VK in the presence of SWNTs. We mention that the same IR spectrum was obtained on PVK bought from Aldrich–Sigma. The main FTIR bands of PVK, peaked at 718, 742, 1122–1156, 1220, 1324, 1404, 1452, 1597 and 1624 cm^{-1}, are attributed to the following vibrations: ring deformation of substituted aromatic structure, CH_2 rocking vibration due to tail to tail addition, C–H in plane deformation of aromatic ring, C–N stretching of VK, C–H in plane deformation of vinylidene group, CH_2 deformation of vinylidene group, ring vibration of VK moiety, C–C + C=C stretching in benzene (B) ring and C–C stretching (B), respectively [36,37]. By adding SWNTs during the bulk polymerization of VK, FTIR spectra of PVK are changed as follows: (i) the intensity of the band peaks at 742 and 1452 cm^{-1} increase; (ii) a new absorption band appears at 1368 cm^{-1}. Taking into account the results reported recently by Kim et al. [38], this band must be associated with the A_2 first order vibration mode of SWNTs; (iii) the intensity ratio between the absorption bands localized at 1368 and 1404 cm^{-1} change in favour of the former; (iv) the band from 1324 shifts to 1334 cm^{-1}. We note that a similar up-shift of the absorption bands at 1334 cm^{-1} has been also reported for the PVK/C_{70} copolymer [39] and (v) the absorption band with the maximum at 1624 cm^{-1} increases monotonically with the amount of SWNTs used in the bulk polymerization of VK. According to Ref. [38], IR absorbance bands of SWNTs are observed at 1170, 1456, 1540 and 1734 cm^{-1}. The absence of the vibrational features of the vinyl group both in SERS (Figs. 3 and 4) and FTIR spectra (Fig. 6) of PVK and of the PVK/SWNTs' composite has to be noticed. The main vibrational features of the vinyl group consist in a Raman line situated at 1644 cm^{-1} and three IR absorbance bands localized at 860, 960 and 1650 cm^{-1}.

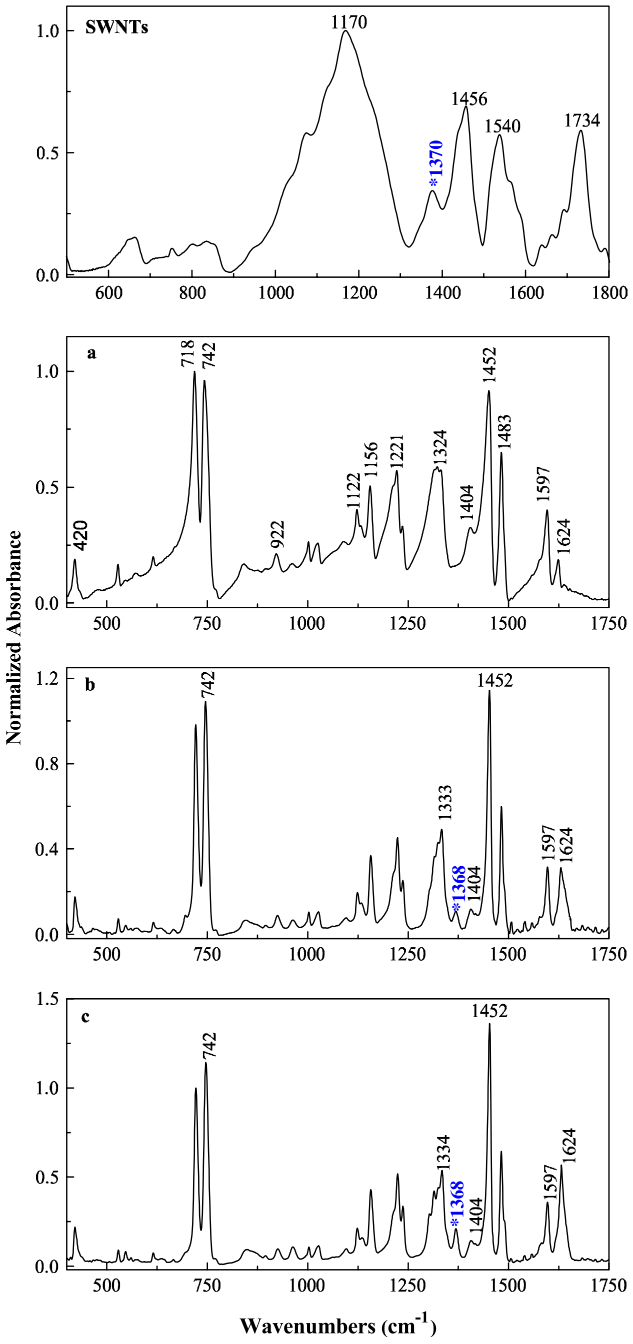

Fig. 6. FTIR spectra of SWNTs, un-doped PVK (a) and the un-doped PVK/SWNTs' composite obtained by bulk polymerization of VK (0.5 g) in the presence of the different CNs weights: 0.01 g (b) and 0.1 g (c).

A careful analysis of above mentioned variations indicates that the main perturbations induced in the chemical structure of PVK by adding SWNTs during the bulk synthesis are in the following vibrations: CH_2 rocking in to tail to tail addition, CH_2 deformation of the vinylidene group, C–H in plane deformation of the vinylidene group, ring vibration of VK moiety and C–C stretching (B). We think that these facts are sufficient to conclude that a covalent attachment of PVK in the un-doped state to SWNTs takes place via the vinyl group. If this conclusion is correct then the electrochemical properties of the pure PVK and the un-doped PVK/SWNTs' composite films immersed in the $LiClO_4$/AN solution must be similar to those reported for electrochemical synthesis of PVK in the presence of CNs. The data shown in Fig. 7 prove the correctness of this hypothesis. TEM images of SWNTs alone and PVK/SWNTs' composite are shown in Fig. 8. Returning to Fig. 7, the two sets of voltammograms presented in Fig. 7a and b are almost identical to those obtained in $LiClO_4$/AN solution, when VK is electrochemically polymerized on a blank Pt plate and a Pt plate coated with SWNTs, respectively [5]. In the former case (Fig. 7a), during the anodic scan, we detect an irreversible oxidation peak at ca. 1.4 V and on the reverse scan, a reduction wave at ca. 0.7 V. In the second case (Fig. 7b), i.e. when the un-doped PVK-functionalized SWNTs' film is deposited on the Pt electrode, the reduction potential peak is down shifted to about 0.56 V and on the anodic scan, an oxidation reaction starts to develop in the potential range (0.8; 1.8) *V* vs. Ag/Ag^+. As a result of the oxidation–reduction reactions, the un-doped PVK-functionalized SWNTs' film colour is changed from light-grey towards green-grey. This experimental fact provides evidence for the

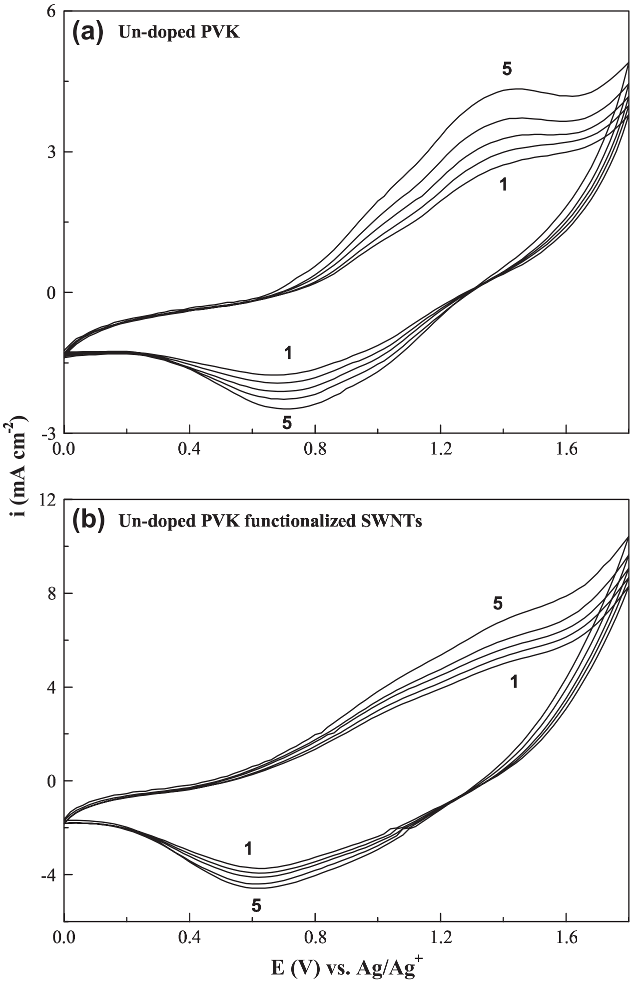

Fig. 7. The first five cyclic voltammograms recorded on the Pt electrode coated with a film of PVK in un-doped state (a) and un-doped PVK-functionalized SWNTs' composite (b), respectively, immersed in the $CH_3CN + LiClO_4$ (10^{-1} M) solution; scan rate = 100 mV s^{-1}.

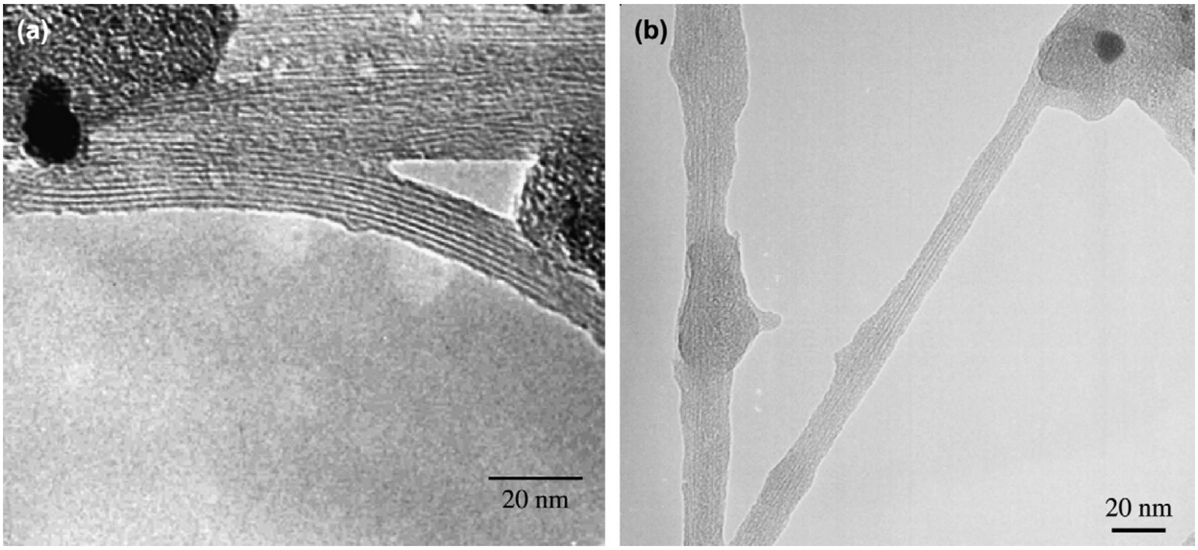

Fig. 8. TEM micrographs of SWNTs (a) and un-doped PVK/SWNTs (b) composite.

passage of PVK from the un-doped state to a doped one. The chemical structure of the un-doped PVK-functionalized SWNTs as well as its oxidation–reduction reaction in the presence of a $LiClO_4$/AN solution is shown in Scheme 2. As a final remark, we note that the proposed chemical structure for the un-doped PVK-functionalized SWNTs is supported by the following experimental facts: (i) the growth of the FTIR band intensity at 1624 cm^{-1} (Fig. 6) as a result of the formation of new C–C bonds between SWNTs and vinylidene group of PVK; (ii) the modification of the intensity ratio of

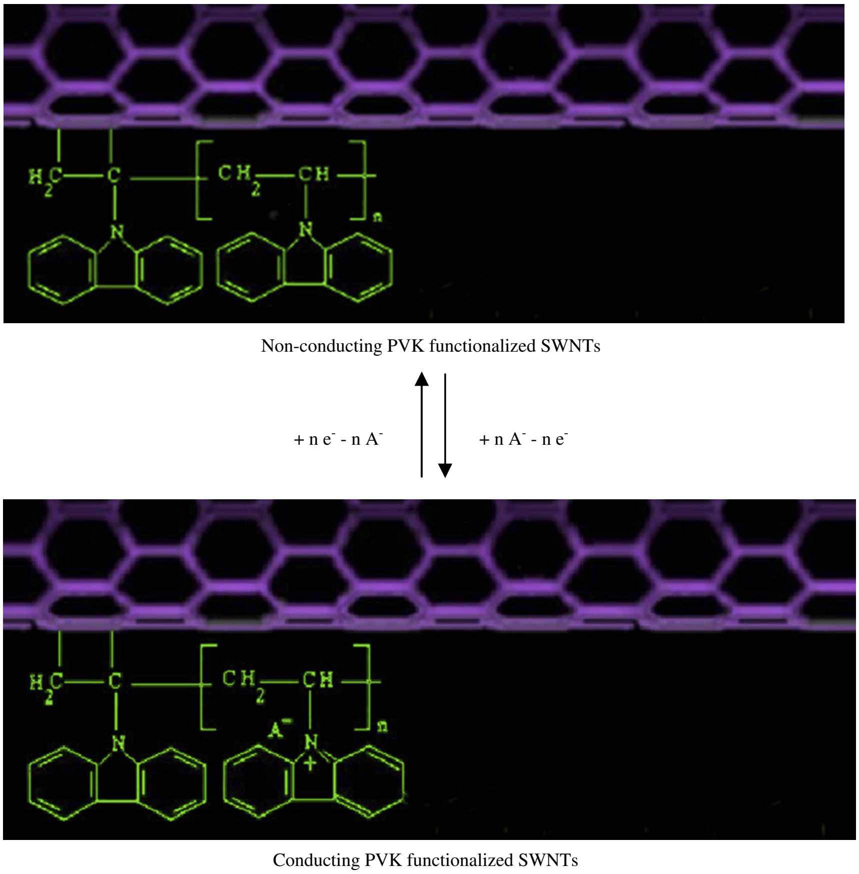

Scheme 2. Electrochemical doping reaction of non-conducting PVK-functionalized SWNTs in the presence of the electrolyte $LiClO_4$ 0.1 M in acetonitrile. $A^- = ClO_4^-$.

Raman lines situated at 162 and 176 cm^{-1} (Fig. 3), as a consequence of an interaction of individual SWNTs with un-doped PVK; (iii) the increase in the intensity of the D band of SWNTs both metallic and semi-conducting (Figs. 2 and 3), after the achievement of the bulk polymerization as a result of the growth of disorder in CNs bundles.

4. Conclusion

This paper reports new results, obtained by photoluminescence, SERS and FTIR spectroscopy concerning the chemical synthesis of the PVK/SWNTs' composite. A new synthesis method has been proposed for the preparation of the composite material based on polymer and carbon nanotubes. A covalent functionalization of SWNTs with PVK in un-doped state is demonstrated by SERS and FTIR spectroscopies. We propose that the bulk polymerization of VK in the presence of SWNTs evolves in the two steps: at the beginning a reaction of addition takes place between SWNTs and VK followed next by the polymerization reaction. In such way, a PVK/SWNTs' composite is obtained, the polymer being in un-doped state. An energy transfer is invoked by photoluminescence spectroscopy, when SWNTs are added to the bulk polymerization of VK. Using cyclic voltammetry, the oxidation–reduction reaction of the PVK-functionalized SWNTs' composite material is also shown.

Acknowledgements

A post-doctoral fellowship to MB by the Spanish Ministry of Science is gratefully acknowledged. Partial funding from the Spanish Ministry of Science and Technology (grant no. MAT 2002-04529-C03) is also acknowledged.

References

[1] Wu W, Li J, Liu L, Yanga L, Guo ZX, Dai L, et al. Chem Phys Lett 2002;364(1–2):196.
[2] Li C, Liu C, Li F, Gond Q. Chem Phys Lett 2003;380(1–2):201.
[3] Wu W, Zhang S, Li Y, Li J, Liu L, Qin Y, et al. Macromolecules 2003;36(17):6286.
[4] Wang W, Li Y, Sun YP. Polymer 2005;46(20):8634.
[5] [a] Baibarac M, Lira-Cantu M, Oro-Sole J, Casan-Pastor N, Gomez-Romero P. SMALL 2006;2(8–9):1075;
[b] Baibarac M, Gomez-Romero P, Lira-Cantu M, Casan-Pastor N, Mestres N, Lefrant S. Eur Polym J 2006;42(10):2302.
[6] Kim JY, Kim M, Choi JH. Synth Met 2003;139(3):565.
[7] Bertoncello P, Notargiacomo A, Erokhin V, Nicolini C. Nanotechnology 2006;17(3):699.
[8] Cadek M, Coleman JN, Barron V, Hedicke K, Blau WJ. Appl Phys Lett 2002;81(27):5123.
[9] Baibarac M, Gomez-Romero P. J Nanosci Nanotechnol 2006;6(2):208.
[10] Tasis D, Tagmatarchis N, Bianco A, Prato M. Chem Rev 2006;106(3):1105.
[11] Biswas M, Haque SA. J Polym Sci Polym Chem 1983;21:1861.
[12] Biswas M, Haque SA. Polym Commun 1985;26:122.
[13] Chen Y, Wang J, Shen J, Cai R, Huang Z. J Polym Sci Polym Chem 1999;37(20):3745.
[14] Liu P. Eur Polym J 2005;41(11):2693.
[15] Biswas M, Gazi MA, Bhagawan SS. Makromol Chem 1978;179:1209.
[16] Ballav N, Biswas M. Synth Met 2005;149(2–3):109.
[17] Lefrant S, Baibarac M, Baltog I, Velula T, Mevellec JY, Chauvet O. Diamond Relat Mater 2005;14(3–7):873.
[18] Baibarac M, Cochet M, Lapkowski M, Mihut L, Lefrant S, Baltog I. Synth Met 1998;96(1):63.
[19] Rivaton A, Mailhot B, Derderian G, Bussiere PO, Gardette JL. Macromolecules 2003;36(15):5815.
[20] Ago H, Petritsch K, Shaffer MSP, Windle AH, Friend RH. Adv Mater 1999;11(15):1281.
[21] Pearson JM, Stoka M. Poly(*N*-vinyl carbazole). Gordon and Breach Science Publishers; 1980. p. 132 [chapter 8].
[22] Dresselhaus MS, Dresselhaus G, Eklund PC. Science of fullerenes and carbon nanotubes. New York: Academic Press; 1996.
[23] Marcoux PR, Schreiber J, Batail P, Lefrant S, Renouard J, Jacob G, et al. Phys Chem Chem Phys 2002;4(11):2278.
[24] Saito R, Dresselhaus G, Dresselhaus MS. Physical properties of carbon nanotubes. London: Imperial College Press; 1998.
[25] Lefrant S, Baltog I, Baibarac M, Schreiber J, Chauvet O. Phys Rev B 2002;65(23):235401.
[26] Rao AM, Richter E, Bandow S, Chase B, Eklund PC, Williams KA, et al. Science 1997;275(5297):187.
[27] Journet C, Maser WK, Bernier P, Loiseau A, Lamy de la Chapelle M, Lefrant S, et al. Nature 1997;388(6644):756.
[28] Pei N, Zhang XT, Li YC, Huang YB, Mo YJ. Vib Spectrosc 1999;21(1–2):39.
[29] Baibarac M, Mihut L, Preda N, Baltog I, Mevellec JY, Lefrant S. Carbon 2005;43(1):1.
[30] Pan H, Liu L, Guo ZX, Dai L, Zhang F, Zhu D, et al. Nano Lett 2003;3(1):29.
[31] Anandhi R, Umapathy S. J Raman Spectrosc 1998;29(11):901.
[32] Lin-Vien D, Colthup NB, Fateley WG, Grasselli JG. The handbook of infrared and Raman characteristic frequencies of organic molecules. Academic Press; 1991. p. 482.
[33] [a] Kojimi Y, Matsuoka T, Takahashi H, Kurauchi T. J Appl Polym Sci 1997;65(13):2782;
[b] Hirsh A, Soi A, Karfunkel JR. Angew Chem Int Ed Engl 1992;31(6):766.
[34] Baibarac M, Baltog I, Lefrant S, Godon C, Mevellec JY. Chem Phys Lett 2005;406(1–3):222.
[35] Heller DA, Barone PW, Swanson JP, Mayrhofer RM, Strano MS. J Phys Chem B 2004;108(22):6905.
[36] Bertoncello P, Notargiacomo A, Nicolini C. Polymer 2004;45(5):1659.
[37] Ballav N, Biswas M. Synth Met 2003;132(2):213.
[38] Kim UJ, Liu XM, Furtado CA, Chen G, Saito R, Jiang J, et al. Phys Rev Lett 2005;95(15):157402.
[39] Cai RF, Bai X, Chen Y, Huang ZE. Eur Polym J 1998;34(1):7.